

Phase transition in the holographic model of superfluidity with backreactions

Yan Peng¹, Xiao-Mei Kuang², Yunqi Liu¹, Bin Wang²

¹ *Department of Physics, Fudan University, Shanghai 200433, China*

² *INPAC, Department of Physics and Shanghai Key Lab for Particle Physics and Cosmology, Shanghai Jiao Tong University, Shanghai 200240, China*

Abstract

In the fully back reacted geometry we develop a supercurrent solution which corresponds to a deformation of superconducting black holes by the spatial component of gauge fields with a non-trivial radial dependence. We investigate the influence of the backreaction on the condensation and the phase structure in the AdS black hole spacetime. Different from that observed in the probe limit, we find that two operators cannot give consistent information on the phase diagram. We argue that only one of these two operators can reflect the real property of the condensation and phase structure in the holographic superconductor. We also generalize our study to the associated phase diagram in the AdS soliton background.

PACS numbers: 04.70.Bw, 74.20.-z

I. INTRODUCTION

The AdS/CFT correspondence [1–3] has provided us a novel way to describe the strongly coupled field theories in a weakly coupled gravitational system. In recent years, it has been found that the gauge gravity duality can be used to provide some insights into superconductivity [4–6]. There exists a gravitational system which closely mimics the behavior of a superconductor. When the temperature of a black hole drops below the critical value, the bulk AdS black hole becomes unstable and scalar hair condenses on the black hole background. The instability of the bulk black hole corresponds to a second order phase transition from normal state to superconducting state and the emergence of the scalar hair in the bulk AdS black hole corresponds to the formation of a charged condensation in the boundary dual CFTs. The gravity models with the properties of holographic superconductors have attracted considerable interest for their potential applications to the condensed matter physics, see for examples [7]–[40].

Recently, the investigation has been further generalized by presenting a DC supercurrent type solution [42, 43]. In terms of AdS/CFT correspondence, the supercurrent states correspond to a deformation of superconducting black holes by the spatial component of the gauge fields with a non-trivial radial dependence. It has been shown that with the introduction of a chemical potential for supercurrent, the critical temperature of the superconducting transition decreases and furthermore at some point the order of phase transition changes from second order to first order. The novel phase diagram brought by the supercurrent is interesting. It further enriches the phase structure observed in the Stückelberg mechanism [24, 34].

In [42, 43] the supercurrent solution was obtained within the approximation scheme of neglecting gravity backreaction. It would be of great interest to examine how the solution changes as we incorporate the gravity backreaction, especially to investigate whether the phase diagram can be modified in the fully back reacted geometry. In the p-wave superfluids system, it was argued that the order of the phase transition depends on the backreaction [44]. The effects of the backreaction on the order of superconducting transition have also been observed in [40, 45, 46]. Here we will further examine how the phase diagram will be modified due to the backreaction in the supercurrent solution in the background of the AdS black hole.

In studying the holographic superconductor, the operator in the dual theory charged under the $U(1)$ is dual to the scalar field ψ in the bulk. At the AdS boundary the asymptotic behavior of the scalar field has the form $\psi \sim \frac{\psi_-}{r^{\lambda_-}} + \frac{\psi_+}{r^{\lambda_+}}$, where $\lambda_{\pm} = (d \pm \sqrt{d^2 + 4m^2l^2})/2$, d is the dimension of the bulk space and

l the AdS radius. Usually the normalizability gives the freedom to consider solutions either with $\psi_- = 0$ or $\psi_+ = 0$. Depending on the choice of boundary conditions, we can read off the expectation value of an operator $\langle O_- \rangle \sim \psi_-$, or of an operator $\langle O_+ \rangle \sim \psi_+$. In order to apply the formalism in gravity to study the real condensed matter physics, one may ask which one of the two possible operators can really reflect the properties of the real condensation. Some works have been reported in examining these two operators in describing the condensations [23, 24, 45, 47]. In [45] it was argued that only one of these two possible operators can reflect the real property of the condensation in the holographic superconductor. This argument was further supported by the investigation in dynamics. In the probe approximation in [42, 43], it was argued that similar behaviors in DC superconductivity and phase structure appear in studying both operators. It is of interest to further examine these two operators in describing the scalar condensation when the fully back reacted geometry is taken into account.

In addition to consider the AdS black hole background, we will also generalize our discussion to the bulk AdS soliton configuration. Including the spatial component of the gauge fields with a non-trivial radial dependence in AdS soliton background, we will examine the scalar condensation and the order of the phase transition between the holographic superconductor and insulator systems. We will compare the effects of the spatial component of gauge fields in the superconducting phase transition in the AdS soliton and AdS black hole backgrounds.

II. THE CONDENSATION IN ADS BLACK HOLE BACKGROUND

A. Equations of motion and boundary conditions

The general lagrangian density describing a $U(1)$ gauge field and a conformally coupled charged complex scalar field in the Einstein gravity background with negative cosmological constant reads [30]

$$L = R + \frac{6}{l^2} - \gamma \left(\frac{1}{4} F^{\mu\nu} F_{\mu\nu} + |\nabla_\mu \psi - i A_\mu \psi|^2 + m^2 |\psi|^2 \right), \quad (1)$$

where l is the AdS radius which will be taken as unity in the following discussion. $\psi(r)$ is the scalar field and A_μ is the Maxwell field. In order to consider the possibility of a DC supercurrent, the vector potential should have both the time component A_t and a spatial component A_x . γ here is the backreaction parameter.

We are interested in including the backreaction, so we use the ansatz of the geometry of the 4-dimensional AdS black hole with the form

$$ds^2 = -r^2 B(r) e^{D(r)} dt^2 + \frac{dr^2}{r^2 B(r)} + r^2 (e^{C(r)} dx^2 + dy^2). \quad (2)$$

There exists an event horizon r_h when $B(r_h) = 0$ and the Hawking temperature reads $T = \frac{r_h^2 B'(r_h) e^{D(r_h)/2}}{4\pi}$. The function $C(r)$ in the metric ansatz is introduced by considering the nonzero x component of the Maxwell field [28].

Assuming the matter fields in the forms

$$\psi = \psi(r), \quad A = \phi(r)dt + h(r)dx, \quad (3)$$

we can obtain equations of motions

$$\psi'' + \left(\frac{4}{r} + \frac{D'}{2} + \frac{C'}{2} + \frac{B'}{B}\right)\psi' + \left(\frac{\phi^2}{r^4 B^2 e^D} - \frac{h^2}{r^4 B e^C} - \frac{m^2}{r^2 B}\right)\psi = 0, \quad (4)$$

$$\phi'' + \left(\frac{2}{r} + \frac{C'}{2} - \frac{D'}{2}\right)\phi' - \frac{2\psi^2}{r^2 B}\phi = 0, \quad (5)$$

$$h'' + \left(\frac{2}{r} + \frac{D'}{2} + \frac{B'}{B} - \frac{C'}{2}\right)h' - \frac{2\psi^2}{r^2 B}h = 0, \quad (6)$$

$$C'' + \frac{1}{2}C'^2 + \left(\frac{4}{r} + \frac{D'}{2} + \frac{B'}{B}\right)C' + \gamma\frac{h'^2}{r^2 e^C} + \gamma\frac{2h^2\psi^2}{r^4 B e^C} = 0, \quad (7)$$

$$B'\left(\frac{2}{r} - \frac{C'}{2}\right) - \frac{1}{2}BD'C' + \frac{6}{r^2}B - \frac{6}{r^2} + \gamma\frac{\phi'^2}{2r^2 e^D} + \gamma\frac{m^2\psi^2}{r^2} + \gamma B\psi'^2 + \gamma\frac{\psi^2\phi^2}{r^4 B e^D} - \gamma\frac{Bh'^2}{2r^2 e^C} - \gamma\frac{h^2\psi^2}{r^4 e^C} = 0, \quad (8)$$

$$D' = \frac{4rC' + r^2C'^2 + 2r^2C'' + \gamma r\left(\frac{2h'^2}{r e^C} + 4r\psi'^2 + \frac{4\psi^2\phi^2}{r^3 B^2 e^D}\right)}{r(4 + rC')}. \quad (9)$$

Considering the symmetry

$$r \rightarrow ar, \quad (x, y, z, \eta) \rightarrow (x, y, z, \eta)/a, \quad \phi \rightarrow a\phi, \quad h \rightarrow ah, \quad (10)$$

we can adjust the solutions to satisfy $r_h = 1$. Since the equations are coupled and nonlinear, we have to numerically integrate these equations from the horizon out to the infinity.

Examining the behavior of the fields near the horizon $r_h = 1$, we find

$$\psi(r) = a + b(r - r_h) + c(r - r_h)^2 + \dots, \quad (11)$$

$$\phi(r) = u(r - r_h) + v(r - r_h)^2 + \dots, \quad (12)$$

$$h(r) = \bar{\alpha} + \bar{\beta}(r - r_h) + \bar{\gamma}(r - r_h)^2 + \dots, \quad (13)$$

$$B(r) = \bar{u}(r - r_h) + \dots, \quad (14)$$

$$D(r) = \bar{v} + \bar{\omega}(r - r_h) + \dots, \quad (15)$$

$$C(r) = \bar{s} + \bar{t}(r - r_h) + \dots. \quad (16)$$

At the AdS boundary, after choosing $m^2 = -2$, the scalar and Maxwell fields behave as

$$\psi = \frac{\psi_-}{r} + \frac{\psi_+}{r^2} + \dots, \quad \phi = \mu - \frac{\rho}{r} + \dots, \quad h = \sigma - \frac{\xi}{r} + \dots \quad (17)$$

The constant coefficients above can be related to physical quantities in the boundary field theory using the AdS/CFT dictionary. μ , ρ are the chemical potential and charge density in the dual theory respectively. ξ is proportional to the current density and σ is the dual current source.

For the value of m^2 we choose, both ψ_- and ψ_+ are normalized. So either ψ_- or ψ_+ can be expectation values of the operators in the field theory $\psi_i \sim \langle O_i \rangle$. In this work we will study both the $\psi_+ = 0$ case and $\psi_- = 0$ case and compare these two operators in the description of the superfluidity.

B. Effects on the phase transition

It was shown in [42, 43] that there exists a first order transition to the normal state in the phase structure at low temperature as the fluid velocity increased. At temperatures close to the critical value T_c , the transition becomes second order. Their results were obtained in the probe approximation and they argued that their results were valid no matter which operator they choose. Here we will examine whether the phase diagram will be modified in the fully back reacted geometry. We will examine the effects of different operators on the condensation and the phase structure when the backreaction is turned on.

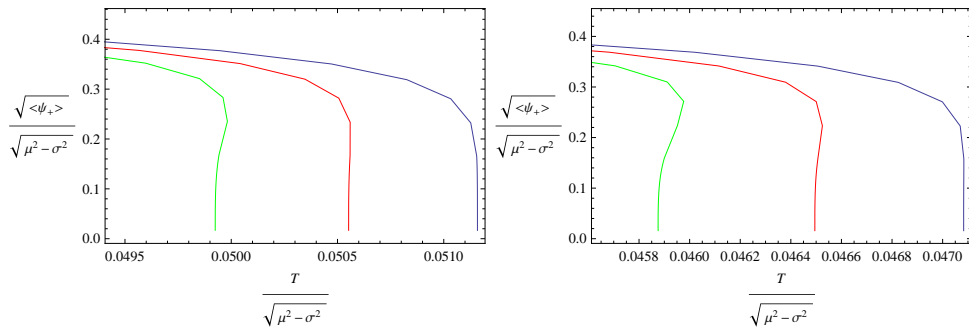


FIG. 1: (Color online) We plot the condensation of the scalar operator $\langle O_+ \rangle$ with the change of the ratio σ/μ . The left panel is for choosing $\gamma = 0$. Lines from right to left are for $\frac{\sigma}{\mu} = 0.26$, $\frac{\sigma}{\mu} = 0.27$ and $\frac{\sigma}{\mu} = 0.28$. The right panel is for choosing $\gamma = 0.1$. Lines from right to left correspond to $\frac{\sigma}{\mu} = 0.21$, $\frac{\sigma}{\mu} = 0.22$ and $\frac{\sigma}{\mu} = 0.23$.

Let us first concentrate on the operator $\langle O_+ \rangle \sim \psi_+$. In Fig.1 we plot the scalar operator as a function of the scaled temperature. Lines from right to left are for the increase of the ratio σ/μ . In the left panel we show that our result is consistent with that observed in [42, 43] when we neglect the backreaction with $\gamma = 0$. We observe that $\langle O_+ \rangle$ does not drop to zero continuously and becomes multivalued when σ/μ is over the critical value 0.27. This phenomenon is attributed to the change of the phase transition from the second order

γ	0	0.2	0.4	0.6
$\frac{\sigma}{\mu}$	0.27	0.19	0.16	0.15

TABLE I: Critical ratio of $\frac{\sigma}{\mu}$ for choosing operator $\langle O_+ \rangle$ with various γ .

to the first order [42, 43]. The right panel is plotted for choosing the backreaction $\gamma = 0.1$. We find the critical $\sigma/\mu = 0.22$. Further increasing the strength of the backreaction, the critical value of σ/μ to accommodate the first order phase transition decreases further as shown in Table I. This tells us that with the increase of the backreaction the first order transition can happen even for smaller fluid velocity. This observation is consistent with that in the Stückelberg mechanism where it was found that with the increase of the backreaction the first order phase transition can be triggered for smaller model parameter in the Stückelberg mechanism [37, 46]. To see clearer of the effect of the backreaction on the phase structure, let us look at Fig.2 where we fixed $\sigma/\mu = 0.22$ with the change of the strength of the backreaction. Again it shows that with the strong enough backreaction, the first order phase transition can happen.

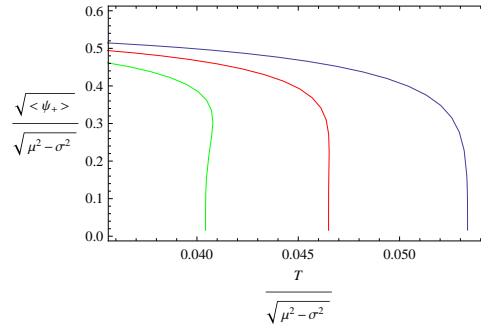


FIG. 2: (Color online) We plot the scalar operator $\langle O_+ \rangle$ as a function of the scaled temperature by fixing $\frac{\sigma}{\mu} = 0.22$. Lines from right to left are for choosing $\gamma = 0$, $\gamma = 0.1$ and $\gamma = 0.2$.

Now let's turn to examine the behavior of the second operator $\langle O_- \rangle \sim \psi_-$. When we neglect the backreaction, the result is shown in the left panel of Fig.3, which is consistent with that reported in [42, 43]. The critical value of σ/μ to trigger the first order phase transition is 0.34. The second operator $\langle O_- \rangle$ exhibits similar behavior to that of the first operator when it comes to DC superconductivity.

When we turn on the backreaction, we find the disagreement of the behaviors of the condensation disclosed by operator $\langle O_- \rangle$ from that of $\langle O_+ \rangle$. With the increase of the strength of the backreaction, the critical values of σ/μ to accommodate the first order phase transition are shown in the right panel of Fig.3 and Table II. The critical value increases when the backreaction becomes stronger, instead of decreasing as shown for the operator $\langle O_+ \rangle$. Furthermore when we fix the ratio σ/μ , the first order phase transition can give way to the second order phase transition with the increase of the backreaction as shown in Fig.4.

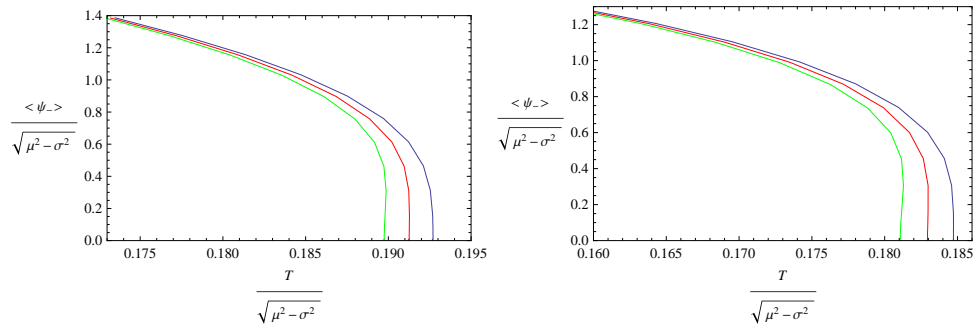


FIG. 3: (Color online) We plot the condensation of the scalar operator $\langle O_- \rangle$ with the change of the ratio σ/μ . The left panel is for choosing $\gamma = 0$. Lines from right to left are for $\frac{\sigma}{\mu} = 0.33$, $\frac{\sigma}{\mu} = 0.34$ and $\frac{\sigma}{\mu} = 0.35$. The right panel is for choosing $\gamma = 0.1$. Lines from right to left correspond to $\frac{\sigma}{\mu} = 0.37$, $\frac{\sigma}{\mu} = 0.38$ and $\frac{\sigma}{\mu} = 0.39$.

γ	0	0.2	0.4	0.6
$\frac{\sigma}{\mu}$	0.34	0.40	0.44	0.47

TABLE II: Critical ratio of $\frac{\sigma}{\mu}$ for $\langle O_- \rangle$ with various γ .

With the backreaction, the drastic different behaviors shown in different operators in the phase diagram bring us the question: which operator is physical and can reflect the real property of the condensation in the superfluidity.

To answer this question, let us do the rescale and plot the figures of the condensation again. Neglecting the backreaction, the condensation behaviors presented by two operators are shown in Fig.5. With the increase of the ratio σ/μ , the condensation gap becomes higher, which means that the scalar hair can be more difficult to be formed in the AdS black hole background. Both operators $\langle O_+ \rangle$ and $\langle O_- \rangle$ present the consistent behaviors in the probe limit. With the increase of the fluid velocity, the critical temperature decreases. This actually agrees with the left panels shown in Fig.1 and Fig.3, where the temperature decreases with the increase of the ratio σ/μ .

Now we replot the condensation for the system with fully backreaction. In Fig.6 the right panel is for the operator $\langle O_+ \rangle$. We find that with the increase of the strength of the backreaction, the gap of the condensation becomes higher and the critical temperature decreases. The condensation gap marks the ease of the scalar hair to be formed [23, 24] and its consistency with the critical temperature indicates that the backreaction hinders the condensation of the scalar field. This property holds no matter the value of the fluid velocity we choose. It is consistent with the effect of the backreaction on the condensation when $A_x = 0$ observed in [30]. In the left panel we show the behavior of the condensation for the operator $\langle O_- \rangle$ in the fully backreacted geometry. We see that for the chosen σ/μ , when the backreaction becomes stronger, the gap of the condensation decreases. However the critical temperature T_c decreases as well with the increase of

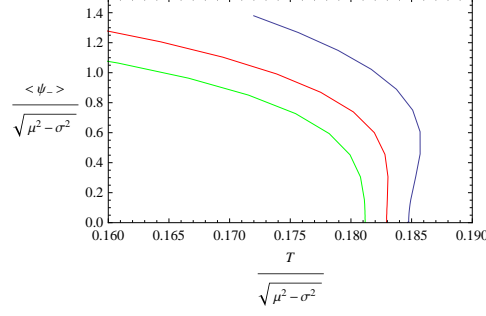


FIG. 4: (Color online) We plot the scalar operator $\langle O_- \rangle$ as a function of the scaled temperature by fixing $\frac{\sigma}{\mu} = 0.38$. Lines from right to left are for choosing $\gamma = 0$, $\gamma = 0.1$ and $\gamma = 0.2$.

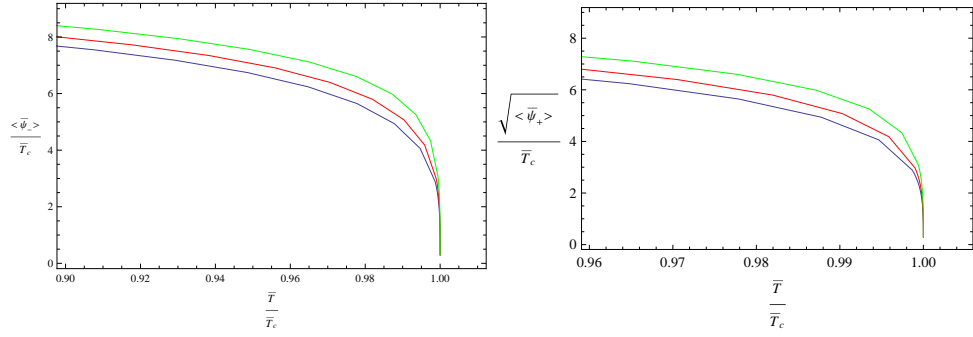


FIG. 5: (Color online) We plot the condensations of operators $\langle O_- \rangle$ (left) and $\langle O_+ \rangle$ (right) in the probe limit. Lines from top to bottom correspond to $\frac{\sigma}{\mu} = 0.23$, $\frac{\sigma}{\mu} = 0.20$ and $\frac{\sigma}{\mu} = 0.17$. In the left panel the critical temperatures for lines from top to bottom are $\bar{T}_c = 0.204$, 0.206 and 0.208 . In the right panel the critical temperatures for lines from top to bottom correspond to $\bar{T}_c = 0.0528$, 0.0543 and 0.0556 .

the backreaction. The effect of the backreaction on the condensation shown by $\langle O_- \rangle$ is different from that when $A_x = 0$. The inconsistency between the condensation gap and the critical temperature tells us that the operator $\langle O_- \rangle$ is not appropriate to describe the condensation. Recall that the expectation value of this operator is related to the asymptotic behavior of the scalar field $\sim 1/r$ at the spatial infinity, which is the same as the operator disclosed incapable of reflecting the correct condensation of the scalar hair in [45, 47].

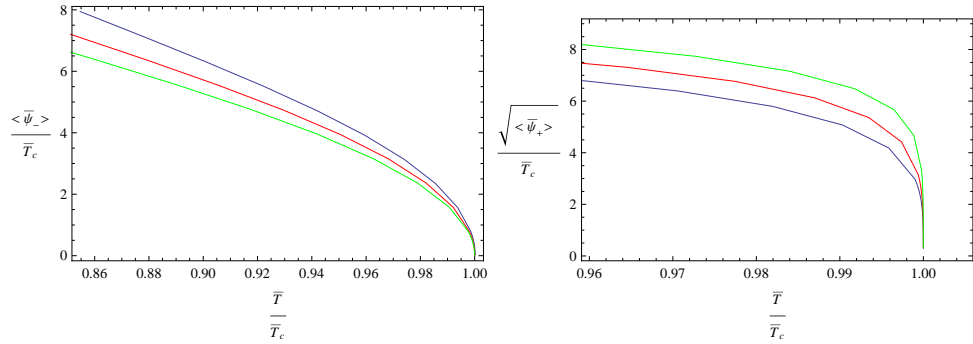


FIG. 6: (Color online) We plot the condensations of operators $\langle O_- \rangle$ (left) and $\langle O_+ \rangle$ (right) with backreactions by fixing $\frac{\sigma}{\mu} = 0.20$. In the left panel the strength of the backreaction for lines from top to bottom are $\gamma = 0$, $\gamma = 0.05$ and $\gamma = 0.1$; and the critical temperatures read $\bar{T}_c = 0.2060$, 0.2051 and 0.2005 . In the right panel lines from top to bottom show $\gamma = 0.1$, $\gamma = 0.05$ and $\gamma = 0$ with the critical temperatures $\bar{T}_c = 0.0476$, 0.0509 and 0.0543 .

Besides the spatial dependence of the vector potential described in (3), it is of interest to examine the result by choosing other forms of the vector potential. In the left panel of Fig.7 we report the result by selecting $A = \phi(r)dt + h(r)dy$. We only concentrate on the operator $\langle O_+ \rangle$. The light grey regions in Fig.7 indicate the second order phase transition and white regions are for the first order phase transition. We see that in the probe limit, the result is consistent with that by choosing (3). Over the critical value of the ratio $\sigma/\mu = 0.27$, the phase transition becomes the first order. When the backreaction is turned on, we see the difference in choosing different vector potential forms. For the comparison, in the right panel of Fig.7 we plot the critical value of σ/μ with the change of backreaction γ for choosing the vector potential in the form of (3). In the left panel we see that when $\sigma/\mu < 0.24$, there is always second order phase transition. When $0.24 < \frac{\sigma}{\mu} < 0.27$, with the increase of γ , the second order phase transition can give way to the first order. For big enough backreaction, there will be another change of the phase structure from the first order to the second order transition. This is consistent with that described in cigar-shaped solution in (3+1)-dimensional AdS spacetime [53]. In the right panel, we observe that when $\frac{\sigma}{\mu} < 0.15$, the phase transition is always of the second order. When $\frac{\sigma}{\mu}$ is in the region $0.15 < \frac{\sigma}{\mu} < 0.27$, the phase transition will change from the second order to the first order. For the vector potential in the form (3), we find that numerical calculation becomes more time consuming when the backreaction becomes stronger. In our computation till $\gamma = 0.6$ we have not observed the change of order of phase transition from the first to the second as shown in the right panel.

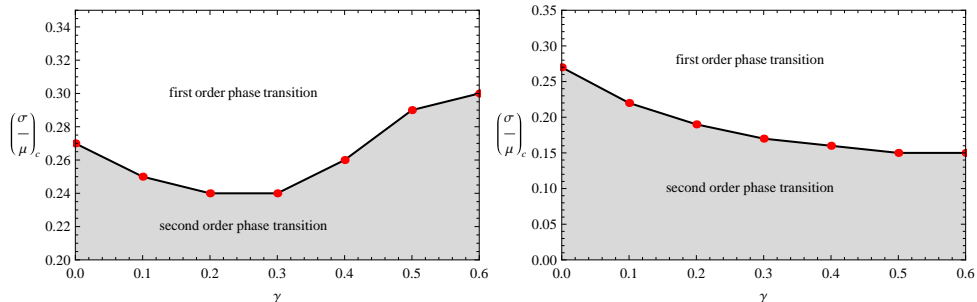


FIG. 7: (Color online) We plot the critical ratio $(\frac{\sigma}{\mu})_c$ with backreaction parameter γ . The left panel is related to the matter fields in the form of $A = \phi(r)dt + h(r)dy$, while the right panel corresponds to the form of (3). The five points from left to right correspond to $\gamma = 0, \gamma = 0.1, \gamma = 0.2, \gamma = 0.3, \gamma = 0.4, \gamma = 0.5$ and $\gamma = 0.6$ respectively and the black lines are obtained by fitting the points in both pictures. The grey fields represent the domain where the second order phase transition happen

III. THE CONDENSATION IN ADS SOLITON BACKGROUND

The holographic duals to the AdS soliton in the Maxwell field with only nonzero vector potential A_t were studied in [16, 24, 30, 41, 46, 48–52]. In the probe limit, it was argued that only the second order phase

transition can happen in the AdS soliton background [24, 48, 54]. In the generalized Stückelberg formalism, it is possible to change the phase transition from the second order to the first order even in the probe limit between the insulator and superconductor in the AdS soliton configuration[46].

It is of interest to generalize our discussion above to the bulk AdS soliton configuration by including the spatial component of the gauge fields with a non-trivial radial dependence. We will examine the scalar condensation and the order of the phase transition between the holographic superconductor and insulator systems.

We use the metric ansatz for the AdS soliton [40]

$$ds^2 = -r^2 e^{C(r)} dt^2 + \frac{dr^2}{r^2 B(r)} + r^2 dx^2 + r^2 B(r) e^{D(r)} d\eta^2, \quad (18)$$

with $B(r)$ vanishes at some radius r_0 , which is the tip of the soliton. In order to get a solution smooth at the tip we require that η to be periodic with a period: $\gamma = \frac{4\pi e^{-D(r_0)/2}}{r_0^2 B'(r_0)}$.

We consider solutions of the forms:

$$\psi = \psi(r), \quad A = \phi(r)dt + h(r)d\eta, \quad (19)$$

With the ansatz of the spacetime, the scalar and Maxwell equations become

$$\psi'' + \left(\frac{4}{r} + \frac{D'}{2} + \frac{C'}{2} + \frac{B'}{B}\right)\psi' + \left(\frac{\phi^2}{r^4 B e^C} - \frac{h^2}{r^4 B^2 e^D} - \frac{m^2}{r^2 B}\right)\psi = 0, \quad (20)$$

$$\phi'' + \left(\frac{2}{r} + \frac{D'}{2} + \frac{B'}{B} - \frac{C'}{2}\right)\phi' - \frac{2\psi^2}{r^2 B}\phi = 0, \quad (21)$$

$$h'' + \left(\frac{2}{r} + \frac{C'}{2} - \frac{D'}{2}\right)h' - \frac{2\psi^2}{r^2 B}h = 0. \quad (22)$$

It is interesting to find that (21) and (22) are similar to (6) and (5), respectively. This similarity will influence the phase structure as we will discuss below.

The nontrivial components of Einstein's equations can be combined into

$$C'' + \frac{1}{2}C'^2 + \left(\frac{4}{r} + \frac{D'}{2} + \frac{B'}{B}\right)C' - \gamma \frac{\phi'^2}{r^2 e^C} - \gamma \frac{2\phi^2\psi^2}{r^4 B e^C} = 0, \quad (23)$$

$$B'\left(\frac{2}{r} - \frac{C'}{2}\right) - \frac{1}{2}BD'C' + \frac{6}{r^2}B - \frac{6}{r^2} - \gamma \frac{h'^2}{2r^2 e^D} + \gamma \frac{m^2\psi^2}{r^2} + \gamma B\psi'^2 - \gamma \frac{\psi^2 h^2}{r^4 B e^D} + \gamma \frac{B\phi'^2}{2r^2 e^C} + \gamma \frac{\phi^2\psi^2}{r^4 e^C} = 0, \quad (24)$$

$$D' = \frac{4rC' + r^2C'^2 + 2r^2C'' + \gamma r\left(\frac{-2\phi'^2}{r e^C} + 4r\psi'^2 - \frac{4\psi^2 h^2}{r^3 B^2 e^D}\right)}{r(4 + rC')}. \quad (25)$$

In contrast to black hole, here we choose the initial boundary condition as:

$$\phi(r) = \tilde{\alpha} + \tilde{\beta}(r - r_0) + \tilde{\gamma}(r - r_0)^2 + \dots, \quad (26)$$

$$h(r) = \tilde{a}(r - r_0) + \tilde{b}(r - r_0)^2 + \dots. \quad (27)$$

The initial forms of the other fields and the expansions of the fields at infinity are the same as the case in back hole.

We can integrate equations numerically from the tip r_0 out to infinity. We will concentrate on the operator $\langle O_+ \rangle$ in our discussion below. There is a critical chemical potential μ_c , above which the scalar hair will be formed as reported in [39, 40]. Neglecting the backreaction, $\gamma = 0$, we observe the behavior of the condensation in the left panel of Fig.8. With the increase of the ratio σ/μ , the condensation gap increases and the critical chemical potential μ_c decreases. This is consistent with the situation we observed in the AdS black hole where μ_c in the soliton plays the similar role to T_c in the black hole. However in the soliton configuration we see that the operator $\langle O_+ \rangle$ drops to zero continuously and the phase transition is always of the second order no matter how big the ratio σ/μ is. This is drastically different from the result seen in the AdS black hole case. For the chosen value of $\frac{\sigma}{\mu}$, the dependence of the condensation on the backreaction is shown in the right panel of Fig.8. The second order phase transition is still kept when the backreaction is taken into account.

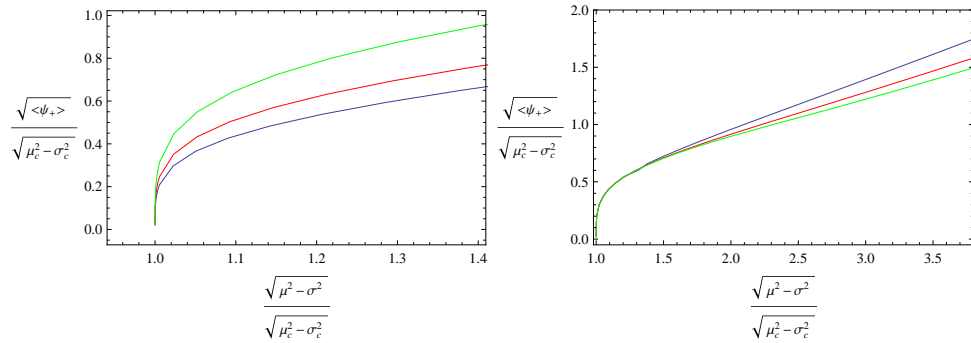


FIG. 8: (Color online) (Left) We plot the condensation with the change of the ratio σ/μ in the probe limit. Lines from top to bottom correspond to $\frac{\sigma}{\mu} = 0.8$, $\frac{\sigma}{\mu} = 0.6$ and $\frac{\sigma}{\mu} = 0$ with the critical values of the chemical potential $\sqrt{\mu_c^2 - \sigma_c^2} = 1.0823, 1.4123$ and 1.7182 respectively. (Right) We fix the ratio $\sigma/\mu = 0.2$. Lines from top to bottom correspond to $\gamma = 0$, $\gamma = 0.6$ and $\gamma = 0.8$ with the critical chemical potential $\sqrt{\mu_c^2 - \sigma_c^2} = 1.6885, 1.6911$ and 1.6920 respectively.

To understand the reason why the spatial component A_x for the vector potential plays different role in the phase diagrams in the AdS black hole and AdS soliton backgrounds, we plot $\phi[u]$ and $h[u]$, where $u = \frac{1}{r}$, in both backgrounds in Fig.9 around the point where the phase transitions begin to happen.

It is clear that in the AdS soliton background the spatial component of the gauge field behaves very different from that in the AdS black hole configuration. The $h[u]$ in the AdS soliton behaves similar to $\phi[u]$ in the black

hole, thus similar to the time component A_t in the AdS black hole, the spatial component in the AdS soliton background cannot bring first order phase transition. On the other hand, $\phi[u]$ in the soliton behaves like $h[u]$ in the black hole background. For this reason, it was observed that only with the time component of the vector potential, the first order phase transition can happen in the five-dimensional AdS soliton background with sufficient backreaction [40], where the charge density and the condensate display sharp discontinuity at the critical of μ . In the four-dimensional AdS soliton background, if we just consider the time dependent of the vector potential, the sharp discontinuity phenomenon in the condensate appears when $\gamma = 0.87$, which indicates the happening of the first order phase transition. The numerical findings is consistent by comparing (21)(22) and (5)(6).

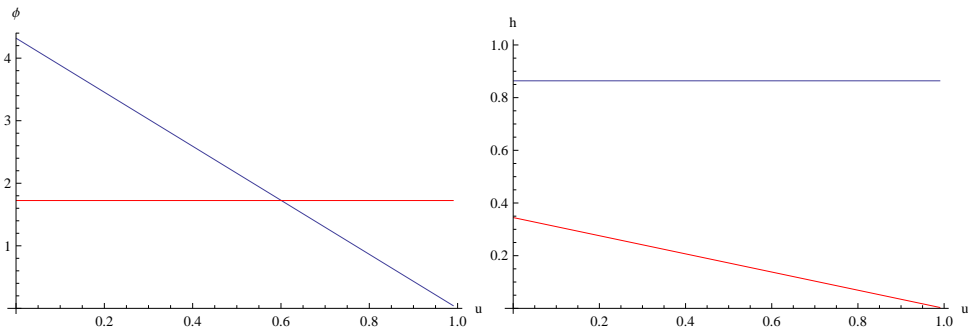


FIG. 9: (Color online) We plot the behaviors of the time component and spatial component of vector potentials in both the AdS black hole and AdS soliton backgrounds. We choose $\gamma = 0.1$, $\frac{\sigma}{\mu} = 0.2$ and $\psi[r_h] = \psi[r_0] = 1/1000$ in plotting these figures. The blue line and red line correspond to the cases in AdS black hole and AdS soliton, respectively.

IV. CONCLUSIONS AND DISCUSSIONS

In this work we have studied a static solution to the system with a charged scalar field coupled to the AdS black hole, which in the dual field theory corresponds to a static current flowing in a superconducting fluid. We have considered the fully back reacted geometry and found the influence of the backreaction on the phase structure. With the backreaction, the first order phase transition can happen for smaller fluid velocity.

Different from that observed in the probe limit [42, 51], when we turned on the backreaction, we found that the condensation behaviors and phase structures reflected from expectation values of different operators are different. This phenomenon was also observed in the study of the effect of the backreaction in the holographic superconductor in [45, 47]. Considering the gap of the condensation which marks the ease of the scalar hair to be formed [23, 24] and its correspondence to the the critical temperature, we concluded that the operator associated with the asymptotic behavior $\sim 1/r$ at the spatial infinity is not appropriate to describe the condensation. This observation is consistent with the findings in [45, 47].

We have further generalized our discussion to the AdS soliton and examined the spatial component of the gauge field on the phase structure in the AdS soliton background. Different from the AdS black hole background, we found that the spatial component of the vector potential cannot bring the first order phase transition in the soliton background. Instead, the first order phase transition can be brought by the time component of the vector potential in the AdS soliton configuration when the backreaction is strong enough as observed in [40, 46]. We have analyzed the reason behind this difference between the AdS black hole and AdS soliton backgrounds.

Acknowledgments

This work has been supported partially by the NNSF of China and the Shanghai Science and Technology Commission under the grant 11DZ2260700.

-
- [1] J. M. Maldacena, *Adv. Theor. Math. Phys.* **2**, 231 (1998).
 - [2] S. S. Gubser, I. R. Klebanov and A. M. Polyakov, *Adv. Theor. Math. Phys. Lett.B* **428**, 105 (1998).
 - [3] E. Witten, *Adv. Theor. Math. Phys.* **2**, 253 (1998).
 - [4] S. A. Hartnoll, *Class. Quant. Grav.* **26**, 224002 (2009).
 - [5] C. P. Herzog, *J. Phys. A* **42**, 343001 (2009).
 - [6] G. T. Horowitz, arXiv:1002.1722 [hep-th].
 - [7] G. T. Horowitz and M. M. Roberts, *Phys. Rev. D* **78**, 126008 (2008).
 - [8] E. Nakano, W. Y. Wen, *Phys. Rev. D* **78**, 046004 (2008).
 - [9] I. Amado, M. Kaminski, and K. Landsteiner, *J. High Energy Phys.* 0905, 021 (2009).
 - [10] G. Koutsoumbas, E. Papantonopoulos, and G. Siopsis, *J. High Energy Phys.* 0907, 026 (2009).
 - [11] O. C. Umeh, *J. High Energy Phys.* 0908, 062 (2009).
 - [12] H. B. Zeng, Z. Y. Fan, and Z. Z. Ren, *Phys. Rev. D* **80**, 066001 (2009).
 - [13] J. Sonner, *Phys. Rev. D* **80**, 084031 (2009).
 - [14] S. S. Gubser, C. P. Herzog, S. S. Pufu, and T. Tesileanu, *Phys. Rev. Lett.* **103**, 141601 (2009).
 - [15] J. P. Gauntlett, J. Sonner, and T. Wiseman, *Phys. Rev. Lett.* **103**, 151601 (2009).
 - [16] R. G. Cai and H. Q. Zhang, *Phys. Rev. D* **81**, 066003 (2010).
 - [17] J. L. Jing and S. B. Chen, *Phys. Lett. B* **686**, 68 (2010).
 - [18] C. P. Herzog, *Phys. Rev. D* **81**, 126009 (2010).
 - [19] S. B. Chen, L. C. Wang, C. K. Ding, and J. L. Jing, *Nucl. Phys. B* **836**, 222 (2010).
 - [20] R. A. Konoplya and A. Zhidenko, *Phys. Lett. B* **686**, 199 (2010).
 - [21] G. Siopsis and J. Therrien, *J. High Energy Phys.* 1005, 013 (2010).
 - [22] K. Maeda, M. Natsuume, and T. Okamura, *Phys. Rev. D* **79**, 126004 (2009).
 - [23] R. Gregory, S. Kanno, and J. Soda, *J. High Energy Phys.* 0910, 010 (2009).
 - [24] Q. Y. Pan, B. Wang, E. Papantonopoulos, J. Oliveira, and A. B. Pavan, *Phys. Rev. D* **81**, 106007 (2010).
 - [25] X. H. Ge, B. Wang, S. F. Wu, and G. H. Yang, *J. High Energy Phys.* 1008, 108 (2010).
 - [26] X. He, B. Wang, R. G. Cai, and C. Y. Lin, *Phys. Lett. B* **688**, 230 (2010).
 - [27] R. G. Cai, Z. X. Nie, B. Wang, and H. Q. Zhang, arXiv:1005.1233 [gr-qc].
 - [28] A. Akhavana and M. Alishahiha, *Rev. D* **83**, 086003 (2011)
 - [29] Y. Brihaye and B. Hartmann, arXiv:1006.1562 (2010).
 - [30] Y. Brihaye and B. Hartmann, *Phys. Rev. D* **81**, 126008 (2010).
 - [31] S. S. Gubser, *Phys. Rev. D* **78**, 065034 (2008).
 - [32] S. A. Hartnoll, C. P. Herzog, and G. T. Horowitz, *Phys. Rev. Lett.* **101**, 031601 (2008).
 - [33] S. A. Hartnoll, C. P. Herzog, and Gary T. Horowitz. *Holographic Superconductors. JHEP*, 12,015,(2008).
 - [34] S. Franco, A. M. Garcia-Garcia, and D. Rodriguez-Gomez, *J. High Energy Phys.* 1004, 092 (2010).
 - [35] S. Franco, A. M. Garcia-Garcia, and D. Rodriguez-Gomez, *Phys. Rev. D* **81**, 041901(R) (2010).
 - [36] F. Aprile and J. G. Russo, *Phys. Rev. D* **81**, 026009 (2010).
 - [37] Q. Y. Pan and B. Wang, *Phys. Lett. B* **693**, 159 (2010).

- [38] X. M. Kang, W. J. Li and Y. Ling, JHEP 1012:069,2010, arXiv:1008.4066[hep-th].
- [39] T. Nishioka, S. Ryu and T. Takayanagi, arXiv:0911.0962v3 [hep-th] 20 Jan 2010.
- [40] G. T. Horowitz and B. Way, arXiv:1007.3714v1 [hep-th] 21 Ju 12010.
- [41] M. Montull, O. Pujolas, A. Salvio, P. J. Silva, arXiv:1105.5392; arXiv:1202.0006.
- [42] C. Herzog, P. Kovtun and D. Son, Phys. Rev. D 79 (2009) 066002.
- [43] P. Basu, A. Mukherjee and H. H. Shieh, Phys. Rev. D 79 (2009) 045010; D. Arean, P. Basu and C. Krishnan, JHEP 10 (2010) 006.
- [44] M. Ammon, J. Erdmenger, V. Grass, P. Kerner and A. OBannon, Phys. Lett. B 686 (2010) 192 [arXiv:0912.3515 [hep-th]].
- [45] Y. Q. Liu, Q. Y. Pan and B. Wang, arXiv:1106.4353(2010).
- [46] P. Yan, Q. Y. Pan, B. Wang, Phys. Lett. B 699 (5) (2011).
- [47] S. A. Hartnoll, C. P. Herzog and G. T. Horowitz, J. High Energy Phys. 12, 015 (2008) [arXiv:0810.1563 [hep-th]].
- [48] T. Nishioka, S. Ryu, and T. Takayanagi, J. High Energy Phys. 03, 131 (2010)
- [49] G. T. Horowitz and B. Way, J. High Energy Phys. 11, 011 (2010).
- [50] A. Akhavan and M. Alishahiha, Phys. Rev. D 83, 086003 (2011) arXiv:1011.6158 [hep-th].
- [51] P. Basu, F. Nogueira, M. Rozali, J. B. Stang, and M. V. Raamsdonk, New J. Phys. 13, 055001 (2011); arXiv:1101.4042 [hep-th].
- [52] Q. Y. Pan, J. L. Jing, and B. Wang, J. High Energy Phys. 11, 088 (2011); arXiv:1105.6153 [gr-qc]
- [53] Y. Brihaye, B. Hartmann, Phys Rev D.83.126008.
- [54] X. M. Kuang, Y. Q. Liu, B. Wang. arXiv:1204.1787v1 [hep-th]